Inorg. Chem. **2003**, *42*, 3685–3692

Complexation of Uranium(VI) and Samarium(III) with Oxydiacetic Acid: Temperature Effect and Coordination Modes

Linfeng Rao,*,† Alexander Yu. Garnov,† Jun Jiang,† Plinio Di Bernardo,‡ PierLuigi Zanonato,‡ and Arturo Bismondo§

Glenn T. Seaborg Center, Lawrence Berkeley National Laboratory, Berkeley, California 94720, Dipartimento di Chimica Inorganica Metallorganica ed Analitica, Università di Padova, via Loredan 4, 35131, Padova, Italy, and Istituto di Chimica Inorganica e delle Superfici del CNR of Padova, Corso Stati Uniti 4, 35127, Padova, Italy

Received March 1, 2003

The complexation of uranium(VI) and samarium(III) with oxydiacetate (ODA) in 1.05 mol kg^{-1} $NaClO_4$ is studied at variable temperatures (25–70 °C). Three U(VI)/ODA complexes (UO_2L, $UO_2L_2^{2-}$, and $UO_2HL_2^{-}$) and three Sm(III)/ODA complexes ($SmL_j^{(3-2j)+}$ with $j = 1, 2, 3$) are identified in this temperature range. The formation constants and the molar enthalpies of complexation are determined by potentiometry and calorimetry. The complexation of uranium(VI) and samarium(III) with oxydiacetate becomes more endothermic at higher temperatures. However, the complexes become stronger due to increasingly more positive entropy of complexation at higher temperatures that exceeds the increase in the enthalpy of complexation. The values of the heat capacity of complexation (ΔC_p° in J K^{-1} mol^{-1}) are 95 ± 6, 297 ± 14, and 162 ± 19 for UO_2L, $UO_2L_2^{2-}$, and $UO_2HL_2^{-}$, and 142 ± 6, 198 ± 14, and 157 ± 19 for SmL^+, SmL_2^-, and SmL_3^{3-}, respectively. The thermodynamic parameters, in conjunction with the structural information from spectroscopy, help to identify the coordination modes in the uranium oxydiacetate complexes. The effect of temperature on the thermodynamics of the complexation is discussed in terms of the electrostatic model and the change in the solvent structure.

1. Introduction

Recently there has been significant interest in the effect of temperature on the coordination of actinides in solution, due to the demands for scientific information to aid the safe management of nuclear wastes.[1−4] It is known that the temperature of nuclear wastes in the storage tanks is significantly above the ambient temperature and can be up to 90 °C. It is estimated that the temperature in the vicinity of the waste form in the repository could be as high as 300 °C. However, the majority of the thermodynamic data on actinide coordination are for 25 °C.[5] The lack of data on actinide coordination at variable temperatures makes it difficult to predict the behavior of actinides in the waste processing and disposal where elevated temperatures are expected.

In addition to providing support to the safe management of nuclear wastes, the study of the effect of temperature on actinide coordination in solution could improve the fundamental understanding of the coordination chemistry of actinides as well. For example, the change in temperature perturbs the structure of solvent in the bulk and in the vicinity of the ions, alters its dielectric property, and thus affects the energetics of the complexation.[6−8] Therefore, the trends in thermodynamic parameters over a wide range of temperature

* Author to whom correspondence should be addressed. E-mail: LRao@lbl.gov. Fax: 510-486-5596.
† Lawrence Berkeley National Laboratory.
‡ Università di Padova.
§ Istituto di Chimica Inorganica e delle Superfici del CNR of Padova.

(1) Wruck, D. A.; Zhao, P.; Palmer, C. E. A.; Silva, R. J. *J. Solution Chem.* **1997**, *26*, 267−275.
(2) Zanonato, P.; Di Bernardo, P.; Bismondo, A.; Rao, L.; Choppin, G. R. *J. Solution Chem.* **2001**, *30*, 1−18.
(3) Jiang, J.; Rao, L.; Di Bernardo, P.; Zanonato, P.; Bismondo, A. *J. Chem. Soc., Dalton Trans.* **2002**, 1832−1836.
(4) Rao, L.; Jiang, J.; Zanonato, P.; Di Bernardo, P.; Bismondo, A.; Garnov, A. Y. *Radiochim. Acta* **2002**, *90*, 581−588.
(5) Martell, A. E.; Smith, R. M. *Critical Stability Constants*; Plenum: New York and London, 1977; Vol. 3; First Suppl., 1982; Second Suppl., 1989.
(6) Seward, T. M. Metal Complex formation in aqueous solutions at elevated temperatures and pressures. In "Chemistry and Geochemistry of Solutions at High Temperatures and Pressures", *Physics and Chemistry of the Earth*, Vols. 13 and 14; Rickard, D. T., Wickman, F. E., Eds.; Pergamon Press: 1981; pp 113−128.

10.1021/ic034227h CCC: $25.00
Published on Web 05/06/2003

could provide insight into the nature of the actinide complex and the solvent effect.

We have started the study of temperature effect on the coordination of lanthanides and actinides with a series of carboxylic acids with different denticity, including acetic,[2,3] malonic,[4] and oxydiacetic acids. The ligands are selected either because they exist in the nuclear wastes as degradation products of more complex organic compounds or because they represent a group of "hard-base" ligands, interactions of which with lanthanides and actinides are expected to be predominantly electrostatic.[8] Previous results on Nd(III) acetate,[2] U(VI)/acetate,[3] and U(VI)/malonate[4] indicate that the enthalpy of complexation is always unfavorable (endothermic) to the complexation and becomes even more unfavorable at higher temperatures. However, the complexes become stronger as the temperature is increased, mainly due to the increasingly larger entropy of complexation at higher temperatures. The increase of entropy with the temperature is interpreted as the consequence of a more disordered bulk water structure at higher temperatures due to the perturbation by thermal movements. In the process of complexation, the solvating water molecules are released to an already expanded and more disordered bulk solvent.[6] As a result, the net gain in the complexation entropy is larger at higher temperatures. Previous results also indicate that the solvation of the ligand plays an important role in determining the energetics of complexation. In the complexation between U(VI) and carboxylates, energy needs to be spent on desolvation of both the metal and the ligand, resulting in endothermic enthalpy and large positive entropy of complexation.

This paper summarizes the results of the complexation of uranium(VI) with oxydiacetate from 25 to 70 °C and Sm(III) with oxydiacetate at 45 and 70 °C. The U(VI) oxydiacetate system has been previously studied at 25 °C,[5,9,10] but not at elevated temperatures. Sm(III) serves as the chemical analogue for trivalent actinides, and its complexation with oxydiacetate was previously studied at a few temperatures up to 50 °C.[11] The present study on the Sm(III) oxydiacetate system extends the temperature range to 70 °C and serves to test the variable-temperature potentiometric and calorimetric setup in our laboratory. Furthermore, due to the unavailability of techniques to characterize the coordination modes, little structural information on the complexes in solution was obtained in the earlier studies. Therefore, the primary objectives in this work are (1) to extend the thermodynamic database for the complexation of U(VI) and Sm(III) with oxydiacetate to elevated temperatures and (2) to provide insight into the nature of the lanthanide/actinide oxydiacetate complexes and the energetics of the complexation, and establish the coordination modes in the complexes. Thermodynamic parameters including formation constants, enthalpy, and entropy were determined by potentiometry and calorimetry. EXAFS was used, in conjunction with the thermodynamic data, to establish the coordination modes in the complexes.

Most recently, a paper in this journal reported structural and thermodynamic data (at 25 °C) on the complexes of U(VI) with oxydiacetic (ODA) and iminodiacetic (IDA) acids in solution.[10] In reviewing the paper, we have found that, while the coordination modes in the U(VI)/IDA complexes are better identified because of the excellent $^{13}C/^{15}N$ NMR data, the coordination modes in the U(VI)/ODA complexes remain ambiguous.[10] More importantly, we have found that the thermodynamic parameters (the enthalpy and entropy of complexation in particular) in the paper[10] are erroneous and should be corrected. Thus, in addition to the primary objectives, our paper is intended to dispute the thermodynamic parameters for U(VI)/ODA complexation in ref 10 published most recently in this journal and present correct thermodynamic parameters to describe the true nature of the U(VI)/ODA system.

2. Experimental Section

2.1. Chemicals. All chemicals were reagent grade or higher. Distilled and deionized water was used in preparations of all the solutions. The stock solutions of samarium perchlorate and uranyl perchlorate were prepared by dissolving samarium oxide (Sm_2O_3) and uranium trioxide (UO_3) in perchloric acid (Sigma-Aldrich, Inc.). The concentration of samarium in the stock solution was determined by EDTA titration complexometry.[12] The concentration of uranium in the stock solution was determined by absorption spectrophotometry and fluorimetry.[13] Gran's potentiometric method[14] was used to determine the concentration of perchloric acid in the stock solutions. Volumetric standard sodium hydroxide solutions were purchased from Brinkmann Instruments, Inc., or Sigma-Aldrich, Inc., and verified to be carbonate-free prior to use. Solutions of sodium oxydiacetate/oxydiacetic acid were prepared by adding calculated amounts of sodium hydroxide into solutions of oxydiacetic acid. The ionic strength of all the solutions used in potentiometry and calorimetry was adjusted to 1.0 mol dm^{-3} at 25 °C by adding appropriate amounts of sodium perchlorate as the background electrolyte.

2.2. Potentiometry. The protonation constants of oxydiacetate (ODA) and the stability constants of the samarium oxydiacetate and uranyl oxydiacetate complexes were determined by potentiometric titrations in a temperature range from 25 to 70 °C. A specially designed titration vessel was used to avoid the problem of water condensation during the titrations at temperatures above the ambient. Details of the titration setup have been provided elsewhere.[2]

Electromotive force (EMF, in millivolts) was measured with a Metrohm pH meter (model 713) equipped with a Ross combination

(7) Schwarzenbach, G. *Interpretation of solution stabilities of metal complexes, in Proc. Summ. Sch. Stability Constants*, 1st; Paoletti, P., Barbucci, R., Fabbrizzi, L., Eds.; Ed. Scient. University of Florence: Florence, Italy, 1977; pp 151−181.
(8) Rizkalla, E. N.; Choppin, G. R. Lanthanides and Actinides Hydration and Hydrolysis. In *Handbook on the Physics and Chemistry of Rare Earths, Vol. 18—Lanthanides/Actinides*: *Chemistry*; Gschneider, K. A., Jr., Eyring, L., Choppin, G. R., Lander, G. H., Eds.; Elsevier Science B.V.: New York, 1994.
(9) Di Bernardo, P.; Tomat, G.; Bismondo, A.; Traverso, O.; Magon, L. *J. Chem. Res. Miniprint* **1980**, 3144−3171.
(10) Jiang, J.; Renshaw, J. C.; Sarsfield, M. J.; Livens, F. R.; Collison, D.; Charnock, J. M.; Eccles, H. *Inorg. Chem.* **2003**, *42*, 1233−1240.
(11) Grenthe, I.; Ots, H. *Acta Chem. Scand.* **1972**, *26*, 1217.
(12) Dean, J. A. *Analytical Chemistry Handbook*; McGraw-Hill: New York, 1995; pp 3−108.
(13) Sill, C. W.; Peterson, H. E. *Anal. Chem.* **1947**, *19*, 646−651.
(14) Gran, G. *Analyst* **1952**, *77*, 661.

pH electrode (Orion model 8102). Because potassium perchlorate is much less soluble than sodium perchlorate, precipitation of the former could result in the clogging of the electrode frit glass septum. As a result, the original electrode filling solution (3.0 mol dm^{-3} potassium chloride) was replaced with 1.0 mol dm^{-3} sodium chloride. The electrode potential (mV) in acidic and basic regions can be expressed as eqs 1a and 1b, respectively. where R is the

$$E = E^\circ + RT/F \ln [H^+] + \gamma_H[H^+] \quad (1a)$$

$$E = E^\circ + RT/F \ln K_w - RT/F \ln [OH^-] + \gamma_{OH}[OH^-] \quad (1b)$$

gas constant, F is the Faraday constant, and T is the temperature. K_w is the ionic product of water (=$[H^+][OH^-]$). The terms of $\gamma_H[H^+]$ and $\gamma_{OH}[OH^-]$ are the electrode junction potentials for the hydrogen and hydroxide ions, respectively. Prior to each protonation or complexation titration, an acid/base titration with standard perchloric acid and sodium hydroxide solutions was performed to obtain the parameters E°, γ_H, and γ_{OH}. These parameters allowed the calculation of hydrogen ion concentrations from the electrode potential in the subsequent titration.

Multiple titrations were conducted at each temperature with solutions of different concentrations (C_{ODA}, C_H, C_{Sm}, or C_U). Fifty to seventy data points were collected in each titration. The protonation constants of oxydiacetate, $K_{H,M}$, and the formation constants of U(VI)−oxydiacetate complexes, $\beta_{j,M}$, on the molarity scale were calculated with the program Superquad.[15] To compare the results at different temperatures, the values of $K_{H,M}$ and $\beta_{j,M}$ were converted to the values on the molality scale, $K_{H,m}$ and $\beta_{j,m}$, based on the method suggested by Grenthe et al.[11]

2.3. Calorimetry. Calorimetry was used to determine the enthalpy of oxydiacetate protonation and complexation with samarium(III) and uranium(VI). Details of the calorimeter (model ISC-4285, Calorimetry Sciences Corp.) were provided previously.[3] The performance of the calorimeter was tested by measuring the enthalpy of protonation of 2-bis(2-hydroxyethyl)amino-2-hydroxymethylpropane-1,3-diol (BIS-TRIS) at different temperatures. The results are -29.1 ± 0.3 kJ mol^{-1} at 45°C and -29.3 ± 0.3 kJ mol^{-1} at 70 °C, compared very well with those in the literature (-28.4 ± 0.3 kJ mol^{-1} at 45 °C and -29.3 ± 0.2 kJ mol^{-1} at 70 °C).[16]

The initial cup solutions (20 cm^3 at 25 °C) usually contained 0.006−0.015 mol dm^{-3} $UO_2(ClO_4)_2$ and $HClO_4$. The titrant was 0.3028 mol dm^{-3} Na_2(ODA)/0.01787 mol dm^{-3} $HClO_4$. At least three titrations with different concentrations of $UO_2(ClO_4)_2$ and $HClO_4$ were conducted at each temperature. For each titration run, n experimental values of the total heat produced in the reaction vessel ($Q_{ex,j}$, $j = 1-n$, usually $n = 50-70$) were calculated as a function of the mass of the added titrant. These values were corrected for the heat of dilution of the titrant ($Q_{dil,j}$), which was determined in separate runs. The net reaction heat at the jth point ($Q_{r,j}$) was obtained from the difference $Q_{r,j} = Q_{ex,j} - Q_{dil,j}$. The quantity Δh_v, the total heat per mole of proton (in protonation titrations) or metal (uranium or samarium in complexation titrations), was calculated by dividing the net reaction heat with the number of moles of proton or metal in the calorimeter vessel. The enthalpy of protonation and complexation was calculated with the computer program Letagrop[17] with Δh_v as the error-carrying variable. Since the enthalpy of acid−base neutralization is needed in the calculation, separate calorimetric titrations were conducted to determine the enthalpy of acid−base neutralization in 1.0 M $NaClO_4$ at variable temperatures. The values are 56.7, 53.9, 52.1, 50.25, and 48.3 kJ mol^{-1} for 25, 35, 45, 55, and 70 °C, respectively.

2.4. Extended X-ray Absorption Fine Structure (EXAFS) Spectroscopy. Two solutions of uranyl oxydiacetate complexes were prepared for EXAFS experiments. The concentrations of U(VI) and oxydiacetic acid (in mmol dm^{-3}) and the pH of the two solutions ($[UO_2(ClO_4)_2]$/[ODA]/pH) are (20/25/2.5) for solution I and (20/200/4.0) for solution II, respectively. Speciation calculations indicate that the 1:1 complex, UO_2(ODA), is dominant (85%) in solution I, and the 1:2 complex, $UO_2(ODA)_2^{2-}$, is dominant in solution II (93%). Approximately 2 cm^3 of the solution was sealed in a polyethylene tube (5 mm i.d.) and mounted on an aluminum sample positioner with Scotch tape for the experiments.

Uranium L_{III} edge EXAFS spectra were collected at the Stanford Synchrotron Radiation Laboratory (SSRL) on wiggler beamline 4-1 under normal ring operating conditions (3.0 GeV, 50−100 mA). Energy scans of the polychromatic X-ray beam were obtained using a Si(220) double-crystal monochromator. The vertical slit width was 0.5 mm, which reduced the effects of beam instabilities and monochromator glitches while providing ample photon flux. The higher order harmonic content of the beam was reduced by detuning the crystals in the monochromator so that the incident flux was reduced to 50% of its maximum at the scan ending energy. The EXAFS data were collected in both the transmission mode using argon-filled ionization chambers and the fluorescence mode using a four-element Ge detector,[18] up to $k_{max} \sim 15$ $Å^{-1}$, which allowed the shell resolution to be about 0.1 Å since $\Delta R \geq \pi/(2k_{max})$.[19] Three and eight scans were performed for solutions I and II, respectively. Energy calibration was based on assigning the first inflection point of the absorption edge for uranium dioxide to 17166 eV. The EXAFS spectra were fit with the R-space X-ray Absorption Package (RSXAP),[20] using parametrized phase and amplitude functions generated by the program FEFF7.[21] Single scattering interactions of $U-O_{ax}$ (axial oxygen) and $U-O_{eq}$ (equatorial oxygen) were included. Inclusion of the multiple scattering interactions of the linear O−U−O unit was found to have negligible effect on the fitting results.

3. Results

3.1. Protonation of Oxydiacetate. The oxydiacetate protonation constants at different temperatures were calculated from the data obtained by potentiometry. These constants were then used in the calculation of the enthalpies of protonation from the data obtained by calorimetry at the same temperature. The results are summarized in Table S1 in the Supporting Information. The values at 25 °C are in good agreement with the available values from the literature.[5]

As shown by the data in Table S1, the enthalpies of protonation of oxydiacetate are positive (endothermic) and increase when the temperature is increased from 25 to 70 °C, indicating that the enthalpy term becomes more unfavor-

(15) Gans, P.; Sabatini, A.; Vacca, A. *J. Chem. Soc., Dalton Trans.* **1985**, 1195−1200.
(16) Smith, R.; Zanonato, P.; Choppin, G. R. *J. Chem. Thermodyn.* **1992**, *24*, 99−106.
(17) Arnek, R. *Ark. Kemi* **1970**, *32*, 81.
(18) Bucher, J. J.; Edelstein, N. M.; Osborne, K. P.; Shuh, D. K.; Madden, N.; Luke, P.; Pehl, D.; Cork, C.; Malone, D.; Allen, P. G.; SRL '95 Conference Proceedings. *Rev. Sci. Instrum.* **1996**, *67*, 1.
(19) Penner-Hahn, B. J. E. *Coord. Chem. Rev.* **1999**, *190−192*, 1101.
(20) (a) Li, G. G.; Bridges, F.; Booth, C. W. *Phys. Rev. B* **1995**, *52*, 6332. (b) *http://lise.lbl.gov/RSXAP*.
(21) Zabinsky, S. I.; Rehr, J. J.; Ankudinov, A.; Albers, R. C.; Eller, M. J. *Phys. Rev. B* **1995**, *52*, 2995.

Table 1. Formation Constants and Corresponding Thermodynamic Parameters[a] for Samarium Oxydiacetate Complexation, $I = 1.05$ mol kg^{-1} ($NaClO_4$)

	T, °C	log $\beta_{j,M}$	log $\beta_{j,m}$	$\Delta G°$ kJ mol^{-1}	$\Delta H°$ kJ mol^{-1}	$\Delta S°$ J K^{-1} mol^{-1}
$Sm^{3+} + L^{2-} = SmL^{+}$	25[b]	5.55 ± 0.07	5.58 ± 0.07	−31.8 ± 0.4	−4.64 ± 0.06	91 ± 2
	45	5.63 ± 0.03	5.66 ± 0.03	−34.5 ± 0.5	−1.88 ± 0.17	102 ± 2
	70	5.67 ± 0.03	5.70 ± 0.13	−37.4 ± 1.0	2.16 ± 0.23	115 ± 4
$Sm^{3+} + 2L^{2-} = SmL_2^{-}$	25[b]	9.89 ± 0.07	9.95 ± 0.07	−56.8 ± 0.4	−12.13 ± 0.06	150 ± 2
	45	9.94 ± 0.03	10.00 ± 0.03	−60.9 ± 0.5	−9.18 ± 0.20	162 ± 2
	70	9.97 ± 0.03	10.03 ± 0.13	−65.9 ± 1.0	−3.1 ± 0.3	183 ± 4
$Sm^{3+} + 3L^{2-} = SmL_3^{3-}$	25[b]	12.79 ± 0.07	12.88 ± 0.07	−73.5 ± 0.4	−17.99 ± 0.06	186 ± 2
	45	12.94 ± 0.03	13.03 ± 0.03	−79.4 ± 0.5	−14.7 ± 0.3	203 ± 2
	70	12.96 ± 0.03	13.05 ± 0.13	−85.7 ± 1.0	−10.4 ± 0.6	220 ± 4

[a] The complex formation constant log $\beta_j = [ML_j^{(3-2j)+}]/([M^{3+}][L^{2-}]^j)$, where $j = 1-3$ and L stands for oxydiacetate. $\beta_{j,M}$ and $\beta_{j,m}$ represent the formation constants on the molarity and the molality scales, respectively. All error limits represent 3σ. [b] From ref 5.

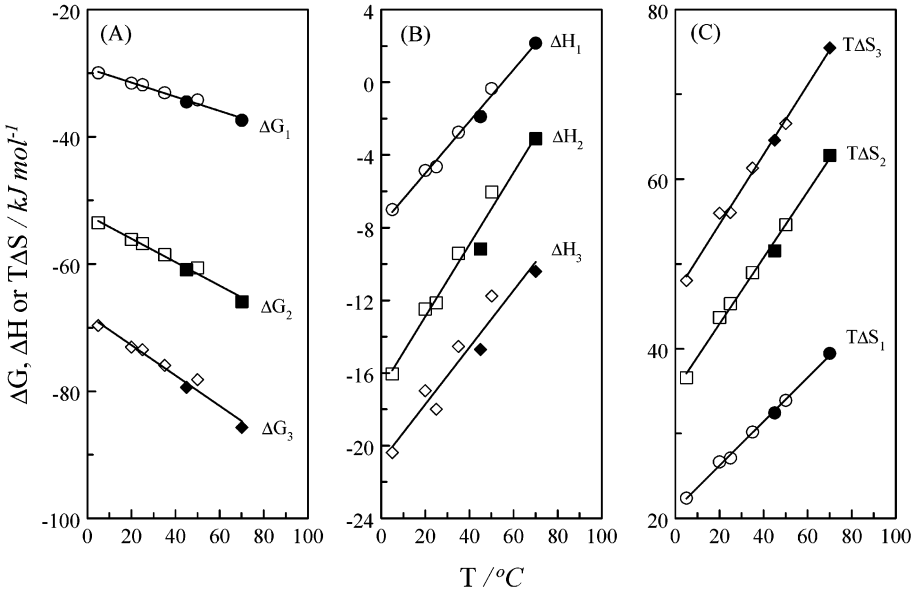

Figure 1. Overall thermodynamic parameters for the complexation of Sm(III) with oxydiacetate. $I = 1.0$ M $NaClO_4$. Solid symbols: data from present work. Open symbols: data from ref 11.

able to the protonation at higher temperatures. Meanwhile, the entropy of protonation increases from 83 J K^{-1} mol^{-1} (25 °C) to 99 J K^{-1} mol^{-1} (70 °C) for HL, and from 132 J K^{-1} mol^{-1} (25 °C) to 163 J K^{-1} mol^{-1} (70 °C) for H_2L, thus enhancing the protonation at higher temperatures. The increase in the entropy term ($T\Delta S$) is slightly larger than the increase in the enthalpy, resulting in a net increase in the protonation constants when the temperature is increased.

3.2. Complexation of Samarium(III) with Oxydiacetate. It was found that the potentiometric and calorimetric data were best fitted with the formation of three consecutive mononuclear complexes, $SmL_j^{(3-2j)+}$ with $j = 1-3$. Table 1 shows the thermodynamic parameters for the complexation of oxydiacetate with Sm(III) at 25, 45, and 70 °C. As shown in Figure 1, the data at 45 and 70 °C from this work compare very well with the values below 50 °C from the literature.[11] These data have not only tested the reliability of our experimental setup for variable-temperature potentiometry and calorimetry but also extended the temperature range from 50 to 70 °C. By assuming linear correlations between $\Delta H°$ and T (Figure 1B), the heat capacity change of the complexation, $\Delta C_{p(SmL_j)}°$ in J K^{-1} mol^{-1}, is calculated to be 142 ± 6, 198 ± 14, and 157 ± 19 for $j = 1$, 2, and 3, respectively.

3.3. Complexation of Uranium(VI) with Oxydiacetate. In contrast to the Sm(III)/ODA system where only ML_j ($j = 1-3$) complexes form, it was found necessary to include a protonated uranyl complex UO_2HL_2 in the model to achieve a reasonably good fit for the potentiometric data from the U(VI)/ODA system. Various combinations of possible species were tried in the fitting, but the best fit was obtained by assuming the formation of three complexes (ML, ML_2, and MHL_2):

$$UO_2^{2+} + L^{2-} = UO_2L^0 \quad (2a)$$

$$UO_2^{2+} + 2L^{2-} = UO_2L_2^{2-} \quad (2b)$$

$$UO_2^{2+} + H^+ + 2L^{2-} = UO_2HL_2^- \quad (2c)$$

Formation constants and Gibbs free energy of complexation are calculated and given in Table 2. The data indicate that the complexation between uranium(VI) and oxydiacetate is enhanced by elevated temperatures. The ML, ML_2, and MHL_2 complexes at 70 °C are 2.3, 3, and 8 times as strong as those at 25 °C, respectively.

The calorimetric titration data are shown in Figure 2, in the form of Δh_v vs $\bar{n}$. The enthalpies of complexation are

Table 2. Formation Constants and Corresponding Thermodynamic Parameters[a] for Uranyl Oxydiacetate Complexation, $I = 1.05$ mol kg^{-1} ($NaClO_4$)

	T, °C	log $\beta_{j,M}$	log $\beta_{j,m}$	$\Delta G°$ kJ mol^{-1}	$\Delta H°$ kJ mol^{-1}	$\Delta S°$ J K^{-1} mol^{-1}
$UO_2^{2+} + L^{2-} = UO_2L$	25	5.01 ± 0.04	5.04 ± 0.04	−28.8 ± 0.2	16.4 ± 0.2	152 ± 1
		5.11 ± 0.01[b]	5.14 ± 0.01[b]	−29.3 ± 0.1	16.86 ± 0.04[b]	155 ± 1[b]
		5.77[c]			26 ± 2[c]	198 ± 12[c]
	35	5.04 ± 0.05	5.07 ± 0.05	−29.9 ± 0.3	18.0 ± 0.2	155 ± 2
	45	5.14 ± 0.09	5.17 ± 0.09	−31.5 ± 0.5	19.3 ± 0.3	160 ± 3
	55	5.31 ± 0.04	5.34 ± 0.04	−33.6 ± 0.3	20.1 ± 0.7	164 ± 3
	70	5.38 ± 0.10	5.41 ± 0.10	−35.5 ± 0.7	20.7 ± 0.5	164 ± 3
$UO_2^{2+} + 2L^{2-} = UO_2L_2^{2-}$	25	7.64 ± 0.07	7.70 ± 0.11	−44.0 ± 0.4	23.8 ± 0.1	227 ± 2
		7.54 ± 0.05[b]	7.60 ± 0.05	−43.4 ± 0.3	23.5 ± 0.1[b]	224 ± 1[b]
		7.84[c]			46 ± 4[c]	304 ± 20[c]
	35	7.67 ± 0.06	7.73 ± 0.06	−45.1 ± 0.4	27.6 ± 0.1	236 ± 2
	45	7.84 ± 0.12	7.90 ± 0.12	−48.1 ± 0.7	31.7 ± 0.2	251 ± 3
	55	8.10 ± 0.06	8.16 ± 0.06	−51.3 ± 0.4	34.9 ± 0.4	263 ± 3
	70	8.12 ± 0.11	8.18 ± 0.11	−53.7 ± 0.7	36.8 ± 0.3	264 ± 3
$UO_2^{2+} + H^+ + 2L^{2-} = UO_2HL_2^-$	25	10.35 ± 0.09	10.44 ± 0.09	−59.6 ± 0.5	22.4 ± 1.4	275 ± 6
		10.03 ± 0.17[b]	10.12 ± 0.17[b]	−57.8 ± 1.0	28.1 ± 0.3[b]	288 ± 4[b]
	35	10.46 ± 0.08	10.55 ± 0.08	−62.2 ± 0.5	22.6 ± 0.1	275 ± 2
	45	10.61 ± 0.13	10.70 ± 0.13	−65.2 ± 0.8	23.4 ± 1.8	278 ± 8
	55	10.93 ± 0.06	11.02 ± 0.06	−69.2 ± 0.4	24.4 ± 0.05	285 ± 2
	70	11.26 ± 0.15	11.35 ± 0.15	−74.6 ± 1.0	30.0 ± 2.2	305 ± 9

[a] The complex formation constant log $\beta = [UO_2H_iL_j^{(2+i-2j)+}]/([UO_2^{2+}][H^+]^i[L^{2-}]^j)$, where L stands for oxydiacetate. β_M and β_m represent the formation constants on the molarity and the molality scales, respectively. All error limits represent 3σ. [b] From ref 9. [c] $I = 0.1$ M KNO_3, from ref 10. The values of ΔH (20 ± 2 kJ mol^{-1}) and ΔS (106 ± 8 J K^{-1} mol^{-1}) for $UO_2(ODA)_2^{2-}$, given in Table 3 of ref 10, are inconsistent with the overall value of log $\beta = 7.84$ in the same table. A careful review of the data in ref 10 suggests that these ΔH and ΔS are probably "stepwise" values. As a result, the overall ΔH and ΔS for $UO_2(ODA)_2^{2-}$ from ref 10 should be 46 ± 4 kJ mol^{-1} and 304 ± 20 J K^{-1} mol^{-1}, which gives a log $\beta \sim 7.8$.

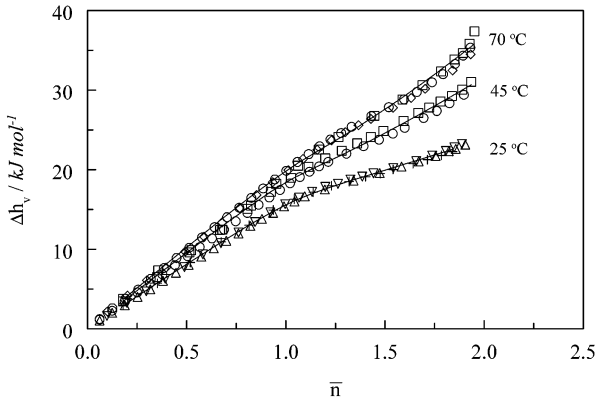

Figure 2. Calorimetric titrations of the U(VI)/oxydiacetate system: Total enthalpy changes per mole of uranium as a function of $\bar{n}$. $I = 1.0$ mol dm^{-3} $NaClO_4$. Titrant: 0.3028 mol dm^{-3} Na_2ODA/0.01787 mol dm^{-3} $HClO_4$. Initial cup volume: 20 mL. Initial cup concentrations (C_U/C_H in mmol dm^{-3}): (□) 5.868/5.981, (○) 9.976/10.167, (◇)14.67/14.95, (+)5.567/5.977, (▽) 9.464/10.161, (△)13.917/14.942.

summarized in Table 2. The molar enthalpy of complexation increases monotonically as the temperature is increased. From these data, the heat capacity change of the complexation, $\Delta C_p°$ in J K^{-1} mol^{-1}, is calculated to be 95 ± 6, 297 ± 14, and 162 ± 19 for the formation of UO_2L, UO_2L_2, and UO_2HL_2, respectively.

Using the thermodynamic values for protonation and complexation in Tables 1 and 3, simulated calorimetric titration curves for 25, 45, and 70 °C were calculated, and they are shown in Figure 2. The excellent agreement between the curves and experimental points at different concentrations confirms the mutual consistency of the calorimetric and potentiometric data on the complexation as well as the reliability of the data on protonation.

The thermodynamic constants (Table 2), enthalpy and entropy in particular, for the complexation of U(VI) with ODA at 25 °C from this work are in good agreement with

Table 3. Best Fit Parameters for Uranium L_{III}-Edge EXAFS

samples	shell	R,[a] Å	N[a]	σ,[b] Å	ΔE_0, eV
solution I:	U−O_{ax}	1.78	2.0	0.0435	−14.12
1:1 uranyl/ODA (85%),	U−O_{eq1}	2.36	3.9	0.0650	−14.12
pH = 2.5	U−O_{eq2}	2.51	1.2	0.0440	−14.12
solution II:	U−O_{ax}	1.78	2.0	0.0426	−11.50
1:2 uranyl/ODA (93%)	U−O_{eq1}	2.35	4.4	0.0851	−11.50
pH = 4.0	U−O_{eq2}	2.51	1.2	0.0592	−11.50
	U−O_{eq3}	2.90	0.8	0.0486	−11.50

[a] The 95% confidence limits for the bond lengths (R) and coordination numbers (N) for each shell are U−O_{ax}, 0.01 Å and ±15%, and U−O_{eq}, 0.02 Å and ±25%, respectively. The amplitude reduction factor $S_0^2 = 1$. [b] σ is the EXAFS Debye−Waller term that accounts for the effects of thermal and static disorder through damping of the EXAFS oscillations by the factor $\exp(-2k^2\sigma^2)$.

the data at 25 °C in the earlier literature,[9] and in excellent trends consistent with the data at other temperatures up to 70 °C. However, these data, especially the enthalpy and entropy of complexation for $UO_2(ODA)$ and $UO_2(ODA)_2^{2-}$, significantly differ from those in a recent paper[10] in this journal. Though the ionic medium in the latter work is different (0.1 M KNO_3), we feel that it does not justify such a big difference. Unfortunately, there is insufficient experimental information in ref 10 to allow determination of the cause of the difference. However, it is noticed that the thermodynamic constants (log $\beta - \Delta H - \Delta S$) for $UO_2(ODA)_2^{2-}$ and $(UO_2)_2(ODA)_2(OH)_2^{2-}$ in Table 3 of ref 10 are not self-consistent. The values of ΔH and ΔS for $UO_2(ODA)_2^{2-}$ and $(UO_2)_2(ODA)_2(OH)_2^{2-}$ (20 and −24 kJ mol^{-1}, 106 and −219 J K^{-1} mol^{-1}) would result in the log β values of 2.03 for $UO_2(ODA)_2^{2-}$ and −7.23 for $(UO_2)_2(ODA)_2(OH)_2^{2-}$, drastically different from the values presented in the same table of ref 10. Furthermore, the difference in enthalpy and entropy between ref 10 and the present work cannot be reconciled due to the unavailability of the information on the calorimetric titration conditions

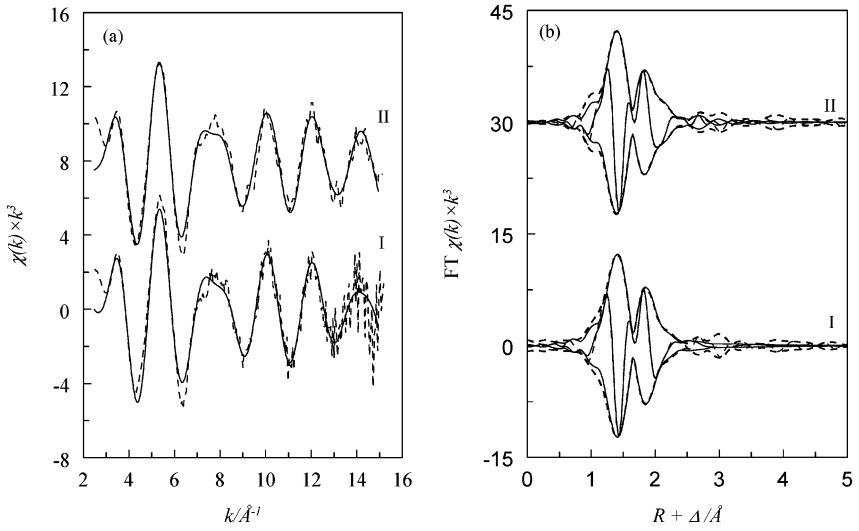

Figure 3. Experimental (dashed lines) and fitted (solid lines) uranium L_{III}-edge EXAFS spectra (a) and associated Fourier transforms (b): (I) solution I, 1:1 U(VI)/ODA complex dominant; (II) solution II, 1:2 U(VI)/ODA complex dominant.

(V^0, $C_U{}^0$, and $C_H{}^0$) and the data processing method in ref 10. However, it is noteworthy that the observed total heat in the calorimetric titrations consists of heats from a number of processes, including protonation/deprotonation of ODA, formation of water due to acid/base neutralization, and formation of a number of U(VI)/ODA complexes. Simultaneously fitting the titration data with all the processes requires at least a number of titrations with different conditions, each consisting of a considerable number of data points. The number of calorimetric titrations and number of data points in each titration (15) in ref 10 seem insufficient. In our study, we have conducted at least three titrations with different concentrations of $UO_2(ClO_4)_2$ and $HClO_4$ at each temperature, with 50−70 points in each titration (see section 2.3 and Figure 2). In addition, we think that, when thermodynamic constants are presented, the corresponding reactions should always be given explicitly, instead of just the composition of the species as shown in Table 3 of ref 10.

3.4. EXAFS. The background-subtracted and k^3-weighted uranium L_{III}-edge EXAFS spectra and corresponding Fourier transform magnitude are shown in Figure 3 (phase shift not corrected). The Fourier transform magnitudes of the two solutions are quite similar in the region of $R < 2$ Å. However, the shoulder at $R > 2.2$ Å becomes more prominent for solution II, suggesting the changes in the coordination sphere and, probably, the presence of additional coordination shell(s). The best fit indicates that both the 1:1 and 1:2 U(VI)/ODA complexes contain two axial oxygens at 1.78 Å, four oxygens at 2.35−2.36 Å, and one oxygen at 2.51 Å (phase shift corrected). In addition, the 1:2 U(VI)/ODA complex (solution II) contains one oxygen at 2.90 Å (Table 3).

4. Discussion

4.1. Effect of Temperature on the Stability of Complexes. There have been discussions in the literature on the use of a Born-type electrostatic model to interpret the effect of temperature on the formation of lanthanide and actinide carboxylate complexes.[2−4] The model predicts the following trends for the electrostatic interaction between species M and L: $\partial(\log \beta)/\partial T > 0$ if $Z_M Z_L < 0$; $\partial(\log \beta)/\partial T < 0$ if $Z_M Z_L > 0$; $\partial(\log \beta)/\partial T = 0$ if $Z_M Z_L = 0$, where β is the complex formation constant and Z_M and Z_L are the electrical charges of the species. We have found that these trends are mostly followed in the formation of 1:1 (ML) complexes. For example, data on 1:1 complexes of Sm(III)/ODA and U(VI)/ODA from this work (Tables 2 and 3), Nd(III)/acetate,[2] U(VI)/acetate,[3] and U(VI)/malonate[4] all show significant increase (1.3−2.8 times) in the stability constants when the temperature is increased from 25 to 70 °C, consistent with the model ($\partial(\log \beta)/\partial T > 0$ if $Z_M Z_L < 0$). However, experimental results of the temperature effect on the formation of 1:2 and/or 1:3 complexes often disagree with the model prediction. For example, for the stepwise formation of the 1:2 (ML_2) U(VI)/ODA complex ($UO_2L^0 + L^{2-} = UO_2L_2{}^{2-}$ where $Z_M Z_L = 0$), the constant shows a slightly upward change while the model predicts $\partial(\log \beta)/\partial T = 0$. Other examples of disagreement between the experimental results and the model have been previously discussed.[4] Because there have been only a few complexation studies at variable temperatures and the available data are too scarce to allow comprehensive tests of the model, cautions should be taken when attempting to predict the temperature effect on complexation by the electrostatic model. More studies of diversified complexation systems covering a wider range of $Z_M Z_L$ are needed.

4.2. Effect of Temperature on the Enthalpy and Entropy of Complexation. Data for the Sm(III)/ODA and U(VI)/ODA systems (Tables 2 and 3) show that, as the temperature is increased, both the enthalpy and entropy of complexation increase, making opposite contributions to the temperature effect on the Gibbs free energy (and thus the overall stability of the complexes). The overall stability constants increase because the increase in the entropy term ($T\Delta S°$) exceeds the increase in the enthalpy. These trends are similar to previous observations for Nd(III)/acetate,[2] U(VI)/acetate,[3] and U(VI)/malonate[4] systems and are ex-

pected for typical hard acid−hard base interactions.[7] The increase of entropy with temperature could be the consequence of a more disordered bulk water structure due to perturbation by more thermal motion at higher temperatures. In the process of complexation, the solvating water molecules are released to a more disordered bulk solvent. As a result, the gain in the complexation entropy is larger at higher temperatures. Detailed discussions were given elsewhere.[2−4,6]

4.3. Coordination Modes in the Oxydiacetate Complexes. 4.3.1. Sm(III)/ODA Complex. For the complexation between ODA and lanthanides, both X-ray crystallographic data for solid state[22] and EXAFS data for solution[23]show that ODA is tridentate in the complexes, with the ether oxygen participating the coordination together with one oxygen from each carboxylate group. In fact, the 1:1 Sm(ODA) complex (log $\beta = 5.55$, Table 1) is much stronger than the bidentate samarium malonate complex (log $\beta = 3.67$)[5] or the 1:2 Sm(acetate)$_2$ complex (log $\beta = 3.36$),[5] in support of a tridentate mode in the lanthanide/ODA complex.

4.3.2. U(VI)/ODA Complex. In contrast to the spherical lanthanide ions, the linear configuration of UO_2^{2+} only allows coordination to occur in or near the equatorial plane, resulting in steric hindrance on multifunctional ligands such as ODA. As a result, ODA may form either a bidentate complex with U(VI) where the ether oxygen does not participate in bonding, or a tridentate complex with the ether oxygen participating in bonding where significant steric tension exists. Some relevant structural data[24,25] for 1:1 and 1:2 U(VI)/ODA solid complexes are shown in Figure 1S in the Supporting Information. The data show that, in solid U(VI)/ODA complexes, a variety of coordination modes are present, including monodentate/bridging (Figure 1Sa), bidentate (Figure 1Sc), and tridentate (Figure 1Sa−c). In fact, the steric tension is manifested in the tridentate solid complexes where the coordinating oxygens are not coplanar. For example, in a three-dimensional solid structure of cross-linked 1:1 U(VI)/ODA complex (Figure 1Sa), the uranyl ions are equatorially surrounded by four carboxylate oxygen atoms and one ether oxygen atom forming an irregular pentagonal bipyramid where the oxygen atoms coordinating to uranium are not exactly in the equatorial plane.[24] A more recent study identified two types of solid structures for 1:2 U(VI)/ODA complexes.[25] In one compound (Figure 1Sb), both ODA ligands are tridentate with two five-membered rings forming a symmetric structure. In another (Figure 1Sc), one ODA is tridentate but the other is bidentate forming an asymmetric structure.

Since there are few structural data in the literature on the U(VI)/ODA complexes in aqueous solutions, the coordination modes in these complexes in solution remain undefined. In this work, we attempt to use the thermodynamic parameters from potentiometry and calorimetry, in conjunction with the structural information from EXAFS, to shed light on the coordination modes in the U(VI)/ODA complexes.

Table 4. Thermodynamic Parameters for the Stepwise Complexation of U(VI) with Dicarboxylate Ligands ($I = 1.0$ M, $T = 25$ °C)

ligand	complex	coordination mode	log K	ΔH kJ^{-1} mol^{-1}	ΔS J K^{-1} mol^{-1}	ref
oxydiacetate	ML	(tridentate?)	5.01	16.4	152	*a*
	ML_2	(bidentate?)	2.63	7.4	75	*a*
thiodiacetate	ML	bidentate	2.96	14.6	105	9
phenylene-1,2-dioxydiacetate	ML	bidentate	2.61	15.8	103	26
malonate	ML	bidentate	5.36	8.0	130	4
	ML_2	bidentate	4.03	3.0	88	4
iminodiacetate	ML	tridentate	8.75	−2.1	161	9

[a] This work.

UO_2L. Table 4 lists the thermodynamic parameters of the complexation between U(VI) and a series of dicarboxylate ligands. It is difficult to compare the enthalpy of complexation among these ligands, because of large variations in the basicities of the carboxylate groups and the ether oxygen, sulfur, and nitrogen atoms. However, the entropy of complexation is much less dependent on such effects and, primarily, reflects dehydration and chelate formation. Data in Table 4 show that the value of $\Delta S°$ (J K^{-1} mol^{-1}) for the 1:1 complex with ODA (152) is similar to that with IDA (tridentate, 161), but significantly higher than those for the bidentate complexes with thiodiacetate (105), phenylene-1,2-dioxydiacetate (103), and malonate (130). It seems that one carboxylate group contributes approximately 50 J K^{-1} mol^{-1} to the overall entropy of complexation. Thus, the thermodynamic data suggest a tridentate mode in the 1:1 U(VI)/ODA complex. This is supported by the data from EXAFS (Table 3). In solution I where the 1:1 complex is dominant, four oxygens are found at 2.36 Å and one oxygen at 2.51 Å. On the basis of the solid structures,[24,25] the oxygen atom at 2.51 Å could be assigned to the ether oxygen in a tridentate ODA ligand, while the four oxygens at 2.36 Å could include two from the carboxylate groups and two from water molecules, not resolved by EXAFS (Figure 4a).

UO_2L_2. It is usually more difficult to reveal the coordination mode in the consecutive second and/or third complexes merely by evaluation of the thermodynamic parameters. However, a comparison of the stepwise formation constants among U(VI)/ODA (log $K_1 = 5.01$, log $K_2 = 2.63$), U(VI)/malonate (log $K_1 = 5.36$, log $K_2 = 4.03$),[4] and Sm(III)/ODA complexes (log $K_1 = 5.55$, log $K_2 = 4.34$) may provide insight into the coordination modes in the complexes. For the latter two systems, the ratio of K_2/K_1 is 1/21 (U(VI)/malonate) and 1/16 (Sm(III)/ODA), respectively, meaning that the second complex is about 1 order of magnitude weaker than the first complex. However, for the U(VI)/ODA system, the second complex is more than 2 orders of magnitude weaker than the first complex ($K_2/K_1 \sim 1/240$). This rather large decrease in the stability of the second U(VI)/ODA complex may imply that the second ODA ligand is probably not tridentate as the first ODA. As a matter of fact,

(22) Albertsson, J. *Acta Chem. Scand*. **1970**, *24*, 3527−3541.
(23) Narita, H.; Yaita, T.; Suzuki, S.; Takai, K.; Tachimori, S.; Motohashi, H. *J. Synchrotron Radiat.* **2001**, *8*, 672−673.
(24) Bombieri, G.; Croatto, U.; Graziani, R.; Forsellini, E.; Magon, L.; *Acta Crystallogr*. **1974**, *B30*, 407−411.
(25) Jiang, J.; Sarsfield, M. J.; Renshaw, J. C.; Livens, F. R.; Collison, D.; Charnock, J. M.; Helliwell, M.; Eccles, H. *Inorg. Chem.* **2002**, *41*, 2799−2806.
(26) Rao, L. F.; Choppin, G. R. *Inorg. Chem*. **1990**, *29*, 3589−3592.

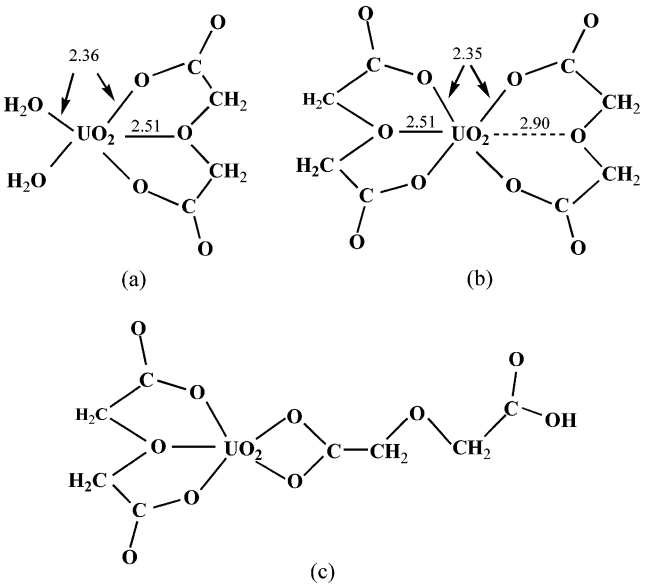

Figure 4. Proposed structures of uranyl oxydiacetate complexes in solution: (a) $UO_2(C_4H_4O_5)$, (b) $UO_2(C_4H_4O_5)_2^{2-}$, and (c) $UO_2(C_4H_4O_5)(HC_4H_4O_5)^-$.

the stepwise entropy for $UO_2(ODA)_2$ (75 J K^{-1} mol^{-1}) is very similar to that for UO_2(malonate)$_2$ (88 J K^{-1} mol^{-1}, Table 4), also suggesting that the second ODA in $UO_2(ODA)_2$ is probably bidentate. An earlier study[9] pointed out that steric hindrance and/or electrostatic repulsion resulting from the crowdedness of two ODA ligands in the equatorial plane might be responsible for the weakening of the second U(VI)/ODA complexes, compared to the malonate complexes. Such steric hindrance and/or electrostatic repulsion could also be the reason that a variety of coordination modes have been observed in the solid state (Figure 1S): tridentate (a−c), bidentate (c), and monodentate/bridging (a).

The EXAFS data for solution II (Table 3) suggest a structure of $UO_2(ODA)_2$ in solution as shown in Figure 4b, which is similar to the solid structure of $UO_2(ODA)_2$ in Figure 1Sc except that the nonbonding ether oxygen in the solution is at a shorter distance (2.90 Å) than in the solid (3.12 Å). This implies that the EXAFS data seem to support the assumption based on the thermodynamic parameters that the second ODA in $UO_2(ODA)_2$ is bidentate. However, since the distance of 2.90 Å is close to the average of the crystallographically determined distances of 2.564 Å (for bonding ether oxygen) and 3.12 Å (for nonbonding ether oxygen), we cannot exclude an alternate assumption that one ether oxygen in the $UO_2(ODA)_2$ complex in solution is in a dynamic mode between bidentate and tridentate configurations. Interestingly, in the same work[25] where solid crystal structures of $UO_2(ODA)_2$ were identified, the EXAFS data on the bulk sample (not a single crystal) of the same material showed that the ether oxygen is at a distance of 2.90−2.95 Å, a median value between the values obtained for the single crystal (Figure 1Sc, 2.564 and 3.12 Å). The authors attributed this discrepancy as reflecting a heterogeneous mixture of symmetric (Figure 1Sb) and asymmetric (Figure 1Sc) coordination.[25,10]

UO_2HL_2. It is difficult to obtain structural information on this species with EXAFS because it is never dominant under the experimental conditions in this work, ranging from 8% to 15%. However, it is reasonable to assume that a partially protonated ODA ligand (HL^-) would prefer a terminal bidentate coordination mode in the complex, leaving the protonated carboxylate group free from metal binding. A structure of the UO_2HL_2 complex is proposed and shown in Figure 4c, where one ODA is coordinated with U(VI) in a terminal bidentate mode similar to that in the uranyl acetate complex described in the literature.[3]

5. Conclusions

In the temperature range from 25 to 70 °C, three samarium oxydiacetate complexes (ML, ML_2, and ML_3) and three uranyl oxydiacetate complexes (ML, ML_2, and MHL_2) were identified by potentiometry and calorimetry. Both the enthalpy and entropy of complexation increase as the temperature is increased, making opposite contributions to the overall stability of the complexes. The complexes become stronger at higher temperatures, due to a larger contribution from the entropy that exceeds the unfavorable effect of enthalpy. The thermodynamic parameters, in conjunction with the structural information from spectroscopy, suggest that ODA is in a tridentate coordination mode in the 1:1 UO_2L complex. However, in the 1:2 UO_2L_2 complex, the second ODA ligand could be either bidentate or in a dynamic mode between tridentate and bidentate coordination configurations. Application and limitations of a Born-type electrostatic model in evaluation of the temperature effect are discussed.

Acknowledgment. This work was supported by the Director, Office of Science, Office of Basic Energy Sciences, Division of Chemical Sciences, under U.S. Department of Energy Contract No. DE-AC03-76SF0098 at Lawrence Berkeley National Laboratory and by the Ministero dell'Università e della Ricerca Scientifica e Tecnologica (MURST, Roma) within the program COFIN00. The EXAFS experiments were conducted at SSRL, which is operated by the Department of Energy, Division of Chemical Sciences.

Supporting Information Available: Table of protonation constants of oxydiacetate and figure depicting structures of uranyl oxydiacetate complexes. This material is available free of charge via the Internet at http://pubs.acs.org.

IC034227H